2014 IEEE/RSJ International Conference on
Intelligent Robots and Systems (IROS 2014)
September 14-18, 2014, Chicago, IL, USA

Torque Control Strategies for Snake Robots

David Rollinson, Kalyan Vasudev Alwala, Nico Zevallos and Howie Choset

***Abstract*— We present three methods of achieving compliant motion with a snake robot by controlling the torques exerted by the joints of the robot. Two strategies command joint torques based solely on the robot's local curvature (i.e. joint angles). A third strategy commands joint angles, velocities, and torques based on the recorded feedback from the robot while executing a previously defined motion under position control. The three control strategies are implemented and compared on a snake robot that includes series elastic actuation (SEA) and torque sensing at each joint, and demonstrate compliant locomotion that adapts automatically to the robot's surrounding terrain.**

I. Introduction

Snake robots, sometimes referred to as hyper-redundant mechanisms [1], consist of actuated links chained together in series. A snake robot's many degrees of freedom give it the potential to navigate a wide range of environments by actively changing its overall shape. However, this same trait makes snake robots difficult to control. Strategies to simplify their control include undulating the robot's joint angles according to parameterized sine waves [2], [3], follow-the-leader controllers [4], and central pattern generators [5].

A limitation of controlling a snake robot via joint angle trajectories is that adapting the trajectories to an irregular environment is difficult. Although our group has had some success in creating adaptive and compliant controllers for snake robots [6], we remain short of replicating the truly versatile locomotion of biological snakes. We feel that this is due in large part to the ability of biological mechanisms to precisely control the forces of their muscles, whereas in robots the precise control of actuator torques is often a challenge. To this end, our group has designed and built the Series Elastic Actuated Snake robot [7], shown in Fig. 1, that has the ability to perform sensitive torque control of its joints.

This work demonstrates that relatively simple controllers applied to the torque of a snake robot's joints, without any other external sensing, can provide significant advantages in overcoming irregular terrain. We outline and present the results of two controllers where torques are commanded based only on the local curvature of the robot. We also present a third method where joint torques and velocities are commanded based on the measured torques and velocities of an existing position-controlled gait.

David Rollinson is a graduate student at the Robotics Institute, Carnegie Mellon University, Pittsburgh, PA, 15213

Kalyan Vasudev Alwala is an undergraduate student in the Dept. of Mechanical Engineering, Indian Institute of Technology Madras, Chennai, TN, 600036

Nico Zevallos is an artist.

Howie Choset is a professor at the Robotics Institute, Carnegie Mellon University, Pittsburgh, PA, 15213

Fig. 1: A photo of the Series Elastic Actuated Snake robot (*SEA Snake*). Each module of the robot has series elastic actuation that enables compliant motion and torque sensing.

II. Related Work

There is significant prior work in controlling snake robots. Hirose's Active Cord Mechanism (ACM) and the formulation of the serpenoid curve [4] established the concept of controlling a snake robot in terms of its backbone curvature and seeking to adapt the robot's shape to its surrounding terrain. Since then recent work in adaptive locomotion for snake robots involves either adjusting the robot's shape based on feedback from tactile sensors [8] or assuming full knowledge of the robot's configuration and the terrain [9], [10]. A thorough survey of modeling and control strategies for snake robots is presented in [11].

An alternative philosophy is to design controllers that adapt to the terrain solely by controlling joint torques, without explicitly sensing the robot's contacts with the world. Our latest snake robot (Fig. 1) consists of modules that each contain a compact series elastic actuator (SEA) [12]. This enables sensitive and stable torque control at each joint, while maintaining the high torque capabilities of geared motors [13]. This work takes the first step in exploiting these unique capabilities to achieve real-world compliant locomotion of a snake robot.

The roll-in-shape controller presented in Section III is an extension of previous position-controlled motions [3], and leverages properties of the 'bellows model' [14] configuration of our snake robots. While the approach to deriving low-impedance gaits in Section V is in its initial stages, it is inspired by similar efforts to learn continuous trajectories

978-1-4799-6934-0/14/$31.00 ©2014 IEEE

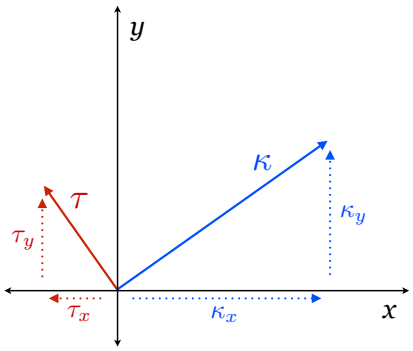

Fig. 2: A visual representation of the roll-in-shape controller. The commanded torque τ is commanded based on the local curvature κ. The commanded torque of the joint is the x or y component of total torque, depending on how the joint is oriented in the robot.

from demonstration for humans and humanoid robotics [15], [16]. The low-impedance sliding controller in Section IV builds on the work of Date et al. [17] and others [18], who demonstrate that a simple torque law based on the derivative of the robot's backbone curvature can propel a wheeled snake over obstacles and through corridors. Kamegawa et al. [19] further extended this approach in simulation for a robot with torque controlled joints and tactile sensing.

III. Compliant Roll-In-Shape

Perhaps the simplest torque-based behavior is one that allows the robot to roll compliantly over the terrain. The ability to roll around the backbone without changing the overall shape is a property of having joints oriented in the lateral and dorsal planes of the robot. Yamada and Hirose discuss this configuration in detail in [14] and refer to the corresponding convention of lateral and dorsal curvatures as a *bellows model*. In particular, they note the relationship between the lateral and dorsal curvatures of the robot κ_x and κ_y and the Frenet-Serret curvature κ to be

$$\kappa^2 = \kappa_x^2 + \kappa_y^2. \tag{1}$$

Intuitively, equation (1) represents how the total local curvature of the of the robot is expressed in terms of its local lateral and dorsal curvatures. If we want to increase or decrease the curvature, the ideal torque to command would be aligned with the curvature. However, if we want to rotate the curvature around the backbone, while changing the curvature as little as possible, the ideal torque command would be orthogonal to the curvature, as visually illustrated in Fig. 2.

As a control law, this results in torques that are a $\frac{\pi}{2}$ rotation from the curvature,

$$\begin{aligned} \tau_x(s) &= -\nu\kappa_y(s) \\ \tau_y(s) &= \nu\kappa_x(s). \end{aligned} \tag{2}$$

In (2), s is the position along the robot's backbone, and ν is a scaling parameter that linearly maps curvature to torque and serves as the torque gain of the controller. The sign of ν can be used to control whether the robot twists clockwise or counterclockwise around its backbone shape. For our initial work we hand-tuned this parameter, and used a value of $\nu = 1.0$ in the results presented in Section VI-A.

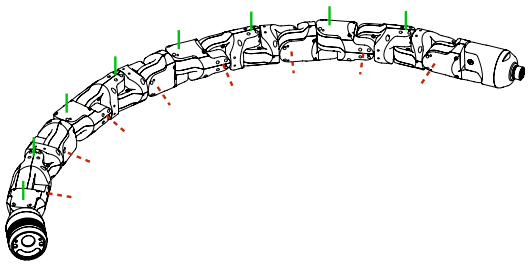

Fig. 3: Diagram of the axes of the snake robot, showing alignment of the robot's joints with the lateral and dorsal planes. The solid and dashed axes indicate actual joints of the robot.

If the robot's joints are evenly spaced along the backbone, this controller can be equivalently written in terms of joint angles, with the parameter ν now scaling between joint angles and torques,

$$\begin{aligned} \tau_x(s) &= -\nu\theta_y(s) \\ \tau_y(s) &= \nu\theta_x(s). \end{aligned} \tag{3}$$

On our snake robots, joints are alternately oriented in the lateral and dorsal planes of the robot, as illustrated in Fig. 3. Because of this, at a given joint we have either a measured θ_x or θ_y, but not both. Since the control law (3) requires knowledge of the joint angle orthogonal to the joint that is being torque-controlled, we linearly interpolate the angle based on the angles of adjacent joints. This interpolation also has the effect of smoothing out the robot's measured curvature.

IV. Empirical Gait Construction

It could be argued that the reason our snake robots move across the ground when executing a gait is less of a result of its shape changes and more of a result of its torques that are applied to cause those shape changes. Since position-controlled gaits are cyclic, when designing them we tend to exploit geometric regularity of the terrain, like flat ground and cylindrical pipes. However with torque-controlled gaits it may be possible that a similar force-based regularity exists that can be exploited for gait design.

Our group, as well as others, have developed a wide range of position-controlled gaits and motions [2], [3] that are useful in the field. While we have had some success in making these gaits adapt to the robot's environment [6], in general the tuning and control of various gaits for a wide range environments is difficult. Therefore, we are interested in methods that could endow our existing library of motions with the low-impedance characteristics that might be enabled by torque control, without starting gait development over from scratch.

To generate low-impedance versions of our existing gaits, we can execute a normal position-controlled gait on the SEA Snake and record the robot's feedback, including joint angles, velocities, and torques. By executing the gait on the nominal

terrain for which the gait was designed (e.g. level ground), we hope to find cyclic velocities and torques that correspond to 'nominal' locomotion. By playing back these positions, velocities, and torques as reference trajectories, and closing the loop primarily on the torques and velocities, we should expect to get a gait that closely mimics the original position-controlled gait on the original terrain and at the same time is more compliant to variations and obstacles.

V. Low-Impedance Sliding

Biological snakes slide through their environment smoothly by pushing off of obstacles. Snake robots have typically achieved similar motions through the use of follow-the-leader joint angle control schemes, often using passive wheels to create an ideal contact with the world [4]. However, when the robot needs to negotiate obstacles or navigate through corridors, these methods can perform poorly. To address these issues, Date [17] proposed using a control law based on the derivatives of local curvatures along the backbone of the snake,

$$\begin{aligned} \tau_x(s) &= \lambda \frac{d(\kappa_x(s))}{ds} \\ \tau_y(s) &= \lambda \frac{d(\kappa_y(s))}{ds}. \end{aligned} \tag{4}$$

In (4), λ is a scaling parameter that maps curvature to torque. This control law will tend to amplify the trends in curvature in a direction along the snake's backbone. The direction of propagation depends on the sign of λ. Intuitively, the commanded torques will be largest at inflection points in the curvature of the snake, as shown in Fig. 4.

As with the roll-in-shape controller, we can again express the desired torques with respect to the robot's joint angles.

$$\begin{aligned} \theta_x'(s) &= \frac{d(\theta_x(s))}{ds} \\ \theta_y'(s) &= \frac{d(\theta_y(s))}{ds}. \end{aligned} \tag{5}$$

We also modify the control law slightly from (4), and command torques proportional to the *square-root* of the derivative curvature,

$$\begin{aligned} \tau_x(s) &= \lambda \ \text{sign}(\theta_x'(s)) \ \sqrt{|\theta_x'(s)|} \\ \tau_y(s) &= \lambda \ \text{sign}(\theta_y'(s)) \ \sqrt{|\theta_y'(s)|}. \end{aligned} \tag{6}$$

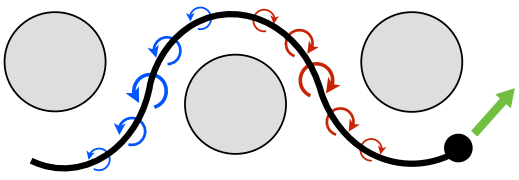

Fig. 4: A visual representation of low-impedance sliding. Torques are commanded based on the derivative of the robot's curvature along the backbone. This has the effect of propagating curves in the robot along the backbone, compliantly sliding around obstacles.

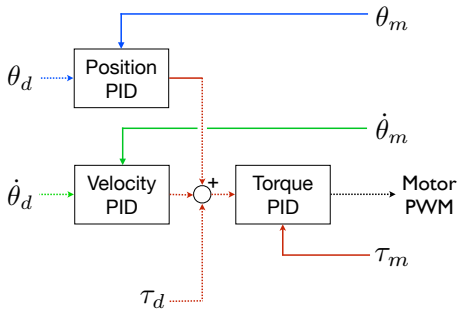

Fig. 5: The control loops on the SEA Snake modules. Position and velocity control loops generate desired torques, which are then combined with a desired feed-forward torque and passed to an inner torque control loop. The measured angle θ_m, velocity $\dot{\theta}_m$, and torque τ_m are all measured directly at the output of the module.

We found that using this square-root relationship, rather than the linear torque relationship proposed by Date [17], provided better locomotion in practice, as it better propagates small curvatures and less aggressively propagates large curvatures. The sign() function above returns 1 or -1, depending on whether its arguments are positive or negative, respectively. This is needed to properly handle square-roots for negative values of $\tau_x(s)$ and $\tau_y(s)$. The derivatives are determined by numerically differentiating and interpolating between adjacent joint angles.

VI. Implementation

The series elastic actuator and low-level controller on each module of our snake robot allows the simultaneous control of desired angular positions, velocities and torques. This is accomplished with a series of PID controllers (Fig. 5), with the inner controller being a torque controller that tracks the measured *output* torque of the module based on the module's sensed spring deflection. A more detailed description of the robot's control architecture can be found in [7].

A. Compliant Roll-In-Shape

To demonstrate the compliant roll-in-shape motion, the robot was driven over various terrains, including people's limbs and bodies. To improve the performance of the robot during rolling, two modifications were made to the control law (3). The first is that the velocities of the joints were damped by commanding a 0 velocity and setting a small proportional gain on the velocity controller on each module. This simulated viscous damping prevents the modules from rolling too quickly when there is little to resist the robot's motion. The second is that the commanded torques were tapered slightly (reduced by 1/3) at the head and tail. This mitigates kinking at the head and tail of the robot, particularly when rolling on flat ground.

A montage of the robot executing compliant roll-in-shape is shown in Fig. 6. The robot easily conforms to the arms and shoulders while rolling under its own power. Figure 7 shows the corresponding commanded and feedback controls from the 8th module, located in the middle of the robot. The top figure shows the orthogonal relation between the commanded

Fig. 6: A montage of the robot undergoing the compliant roll-in-shape motion. The robot actively rolls along while compliantly adapting its shape to match its surroundings.

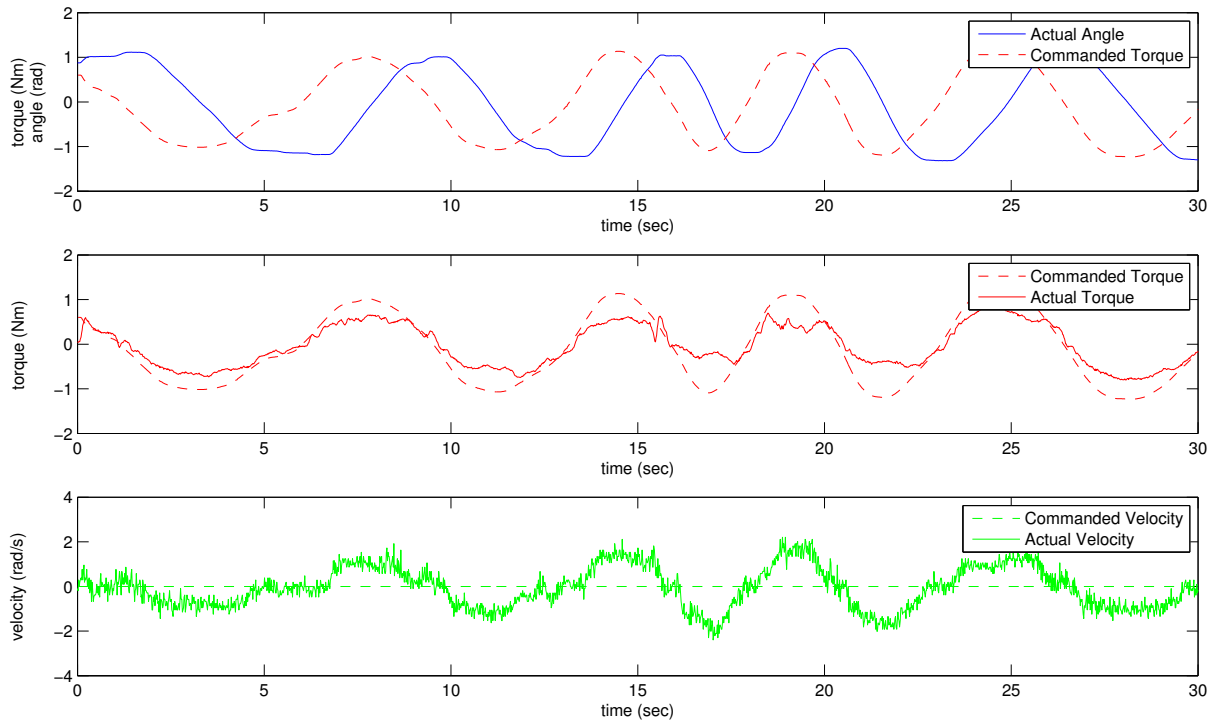

Fig. 7: Commanded and feedback data from one of the robot's doing the motions shown in Fig. 6. The top plot shows the relationship of the commanded torque to the joint angle. The middle plot shows the commanded vs. measured torque output of the module. The bottom plot shows the module's commanded and measured velocity. Note that the robot's cyclic rolling motion tends to speed up and slow down over time, since the shape changes result solely from the commanded joint torques interacting with the surrounding terrain.

torque and the robot's joint angle, indicated by the $\frac{\pi}{2}$ phase shift between the two, as well as the slight smoothing effect from interpolating joint angles for the controller. The middle plot shows the module's tracking of commanded torque, where the effect of the viscous damping due to a commanded zero velocity can be observed.

B. Empirical Gait Construction

We demonstrated the empirical construction of low-impedance gaits with the slithering gait [3]. This motion is designed for flat ground, and is a modified version of sinus-lifting [2] where the motion gradually tapers at the head of the robot so that the camera image remains steady during locomotion.

The gait was executed on the SEA snake and the feedback from each of the robot's modules was recorded at 100 Hz. Before using the feedback as a reference trajectory, the torque and velocity trajectories for each module were smoothed with a forward-back rolling window (Matlab's `smooth` function) to remove high-frequency noise without introducing lag into the trajectory. The gains on the module controllers were set such that the position gains were much lower compared to the velocity and torque gains.

During the execution of low-impedance slithering, the robot was able to navigate an abrupt bend using only the nominal feedforward motion, as shown in Fig. 8 and the accompanying video. Figure 9 shows the feedback from the 6th module in the robot as it negotiated the bend. Note the significant deviation in the measured joint angle away from the commanded trajectory, designed to move the robot in a straight line. Instead of generating large torques to maintain the commanded joint angle, the joint tracked primarily the torque and velocity trajectories, enabling the robot to accept the deformations and gradually return to its reference trajectory afterwards.

Fig. 8: A montage of the robot undergoing the a low-impedance slithering gait. The robot executes the gait cycle and progress forward, but can be easily deformed form the nominal shape. This allows the robot to progress around a bend that would not have been possible with a standard position-controlled gait.

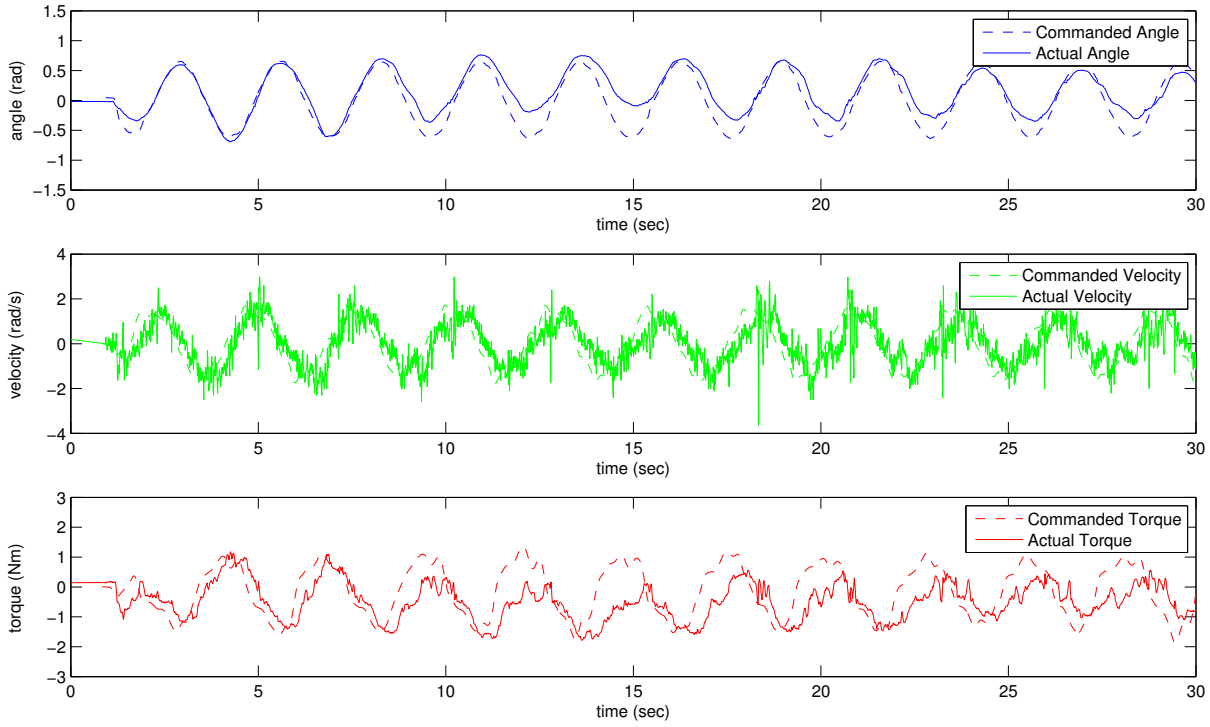

Fig. 9: Commanded and feedback data from robot's 6th module for the above trial of low-impedance slithering. The robot primarily tracks the commanded torque and velocity. This allows the joint angle to deviate significantly from its commanded value without introducing large torques or corrections. Unlike compliant roll-in-shape, the cyclic motions of the commands remains steady throughout the trial, due to the feedforward gait controller.

Also of note in Fig. 9 (and Fig. 7) is the noise in the velocity feedback from the snake robot. This is because the joint's velocity measurement is derived by numerically differentiating the module's absolute magnetic encoders. This noise presents a practical upper limit on the gain that can be set for tracking velocity, but for gain levels used for these low-impedance controllers it is not problematic.

C. Low-Impedance Sliding

To initially demonstrate low-impedance sliding, the robot progressed through a set of rounded obstacles in a corridor. As with the roll-in-shape controller, the velocities of the joints were damped, and commanded torques were tapered slightly towards the head and tail. To decrease the coefficient of friction and smooth out the robot's shape, we covered the body with nylon cable braid.

In order to initiate curvature to propagate down the backbone, the torque of first joint was oscillated with a fixed frequency,

$$\tau_{head} = A\, sin(\omega t). \tag{7}$$

This allowed for compliance similar to the rest of the modules while propagating high amplitude waves through the backbone curvature. Even with the implementation of this simple controller, the robot was able to successfully negotiate the obstacles in a surprisingly life-like manner, as shown in Fig. 10 and the supporting video. Although this method of blindly oscillating the torque of the head module is compliant to the surrounding environment, it should be noted that it is an extremely naive way of setting and propagating the sliding motion. It often results in erratic behavior, like the robot turning around at the end of Fig. 10.

In order to steer heading direction and the overall motion of the robot, we can instead control the head module's joint angle,

$$\theta_{head} = A_\theta \, sin(\omega t) + \epsilon. \quad (8)$$

In (8) A_θ is the amplitude, ϵ is offset and ω is a fixed frequency of oscillation. ϵ is used to steer the head module and thereby control the direction of the robot. A_θ is used to begin and sustain oscillations in the robot in the cases of low backbone curvature as well as maintain some of the open-loop controller's ability to wriggle past obstacles.

This controller was tested in a random field of 5 cm (2 in) peg obstacles, shown in Fig. 11. The parameters A_θ and ϵ were controlled by an operator in real time using a joystick. The resulting head joint angles and the values of A_θ and ϵ are shown in Fig. 12. Using this manual controller, we inferred that the head angle offset, ϵ, is by itself sufficient to control the heading direction of the robot, but that some baseline oscillation, $A_\theta > 0$, was needed to reliably propel the robot forward. We have also intuitively inferred that A_θ and ϵ together can be used to control the radius of turning during locomotion.

VII. Conclusions and Future Work

Torque control is a vital component to achieving adaptive and compliant motions with any robot. For snake robots we have presented three different torque control strategies that have been implemented on a physical snake robot. With all of the controllers, the robot was able to actively adapt to its surrounding environment, even without tactile sensing or any other form of exteroceptive sensing. With a simple manual controller, we were able to intuitively steer the robot through an irregular test environment. That said, this work is in a very preliminary stage, and future work is continuing on all three methods.

A. Compliant Roll-In-Shape

The controller presented in Section III depends solely on the curvature of the robot along its backbone and serves as a general starting point for creating more complex motions. One interesting avenue of future work will involve tuning the commanded torque based on the overall shape of the robot. For example, a useful motion could be rolling along the ground but being compliant to small obstacles like rocks and gaps. The controller presented here tends to wrap the robot around obstacles, rather than roll over them. One strategy to address this issue could involve adjusting the desired torques to allow tighter curvatures in one dimension and stiff curvatures in an orthogonal dimension, based on the robot's overall shape [20]. Alternatively, the torques could also be adjusted based on the estimated pose of the robot [21].

B. Empirical Gait Construction

We presented initial results in constructing a low-impedance version of the slithering gait. Although limited, this identical approach can be applied to other position-controlled gaits or motions. Future work will involve generalizing and parameterizing these new low-impedance motions, so that they can be easily adjusted online, like traditional position-controlled gaits the we currently use. To do this, we intend to draw on existing work that has focused on learning continuous trajectories and controllers from demonstration for humans and humanoid robots [15], [16].

C. Low-Impedance Sliding

This control strategy is extremely interesting because it seems to closely mimic the motions of biological snakes [22]. The simple controller presented in Section V works well in confined spaces, but tends to perform poorly when the shape is not well-constrained. One possible solution could be to develop schemes that shift from executing the sliding motion to executing feedforward gaits like those in Section IV, depending on the presence of obstacles. Work is also underway to incorporate other sensor data such as IMUs and encoders to automatically adjust the head steering parameters. Finally, we are working on combining the commanded torque (7) and position (8) functions for steering the head module into a unified function which controls the direction of the robot, while at the same time allowing head of the robot to be compliant.

The characteristics of the skin of the snake also play an extremely important role during sliding motion [22]. We are investigating other low-friction, or possibly directional-friction, skins to aid in sliding over a wider range of surfaces. If coupled with forms of active propulsion along the spine of the robot, like tracks or small wheels, it is possible that this sliding control strategy could provide exceptional mobility over rough terrain.

VIII. Acknowledgements

The authors would like to thank Leif Jentoft and Gill Pratt for their work in simulating low-impedance torque control for snake robots, which laid the groundwork for most of Section IV. This work was funded by the DARPA M3 program.

References

[1] G. Chirikjian and J. Burdick, "The kinematics of hyper-redundant robot locomotion," *IEEE Transactions on Robotics and Automation*, vol. 11, no. 6, pp. 781–793, 1995.

[2] H. Ohno and S. Hirose, "Design of slim slime robot and its gait of locomotion," *Proceedings 2001 IEEE/RSJ International Conference on Intelligent Robots and Systems.*, pp. 707–715, 2001.

[3] M. Tesch, K. Lipkin, I. Brown, R. L. Hatton, A. Peck, J. Rembisz, and H. Choset, "Parameterized and Scripted Gaits for Modular Snake Robots," *Advanced Robotics*, vol. 23, pp. 1131–1158, June 2009.

[4] S. Hirose, *Biologically Inspired Robots*. Oxford University Press, 1993.

[5] A. J. Ijspeert, "Central pattern generators for locomotion control in animals and robots: a review.," *Neural Networks*, vol. 21, pp. 642–53, May 2008.

[6] D. Rollinson and H. Choset, "Gait-Based Compliant Control for Snake Robots," in *IEEE International Conference on Robotics and Automation (ICRA)*, (Karlsruhe, Germany), pp. 5123–5128, 2013.

[7] D. Rollinson, Y. Bilgen, B. Brown, F. Enner, S. Ford, C. Layton, J. Rembisz, M. Schwerin, P. Velagapudi, A. Willig, and H. Choset, "Design and Architecture of a Series Elastic Snake Robot," in *IEEE/RSJ International Conference on Intelligent Robots and Systems (IROS)*, (Chicago, USA), IEEE/RSJ, 2014.

[8] P. Liljeback, K. Pettersen, O. Stavdahl, and J. Gravdahl, "Experimental Investigation of Obstacle-Aided Locomotion With a Snake Robot," *Robotics, IEEE Transactions on Robotics*, vol. 27, no. 4, pp. 792–800, 2011.

Fig. 10: A montage of the low-impedance sliding motion, with an open-loop head oscillation to initiate motion. The robot undulates until the shape of the robot closely matches the shapes of the buckets and the snake slides through. Afterwards, the head continues to oscillate, causing the robot to turn in place.

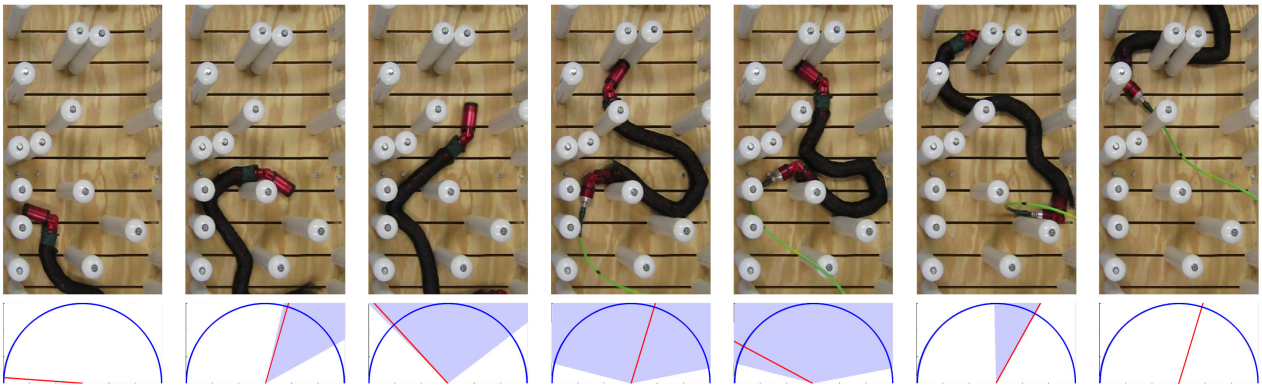

Fig. 11: A montage of the guided head low-impedance sliding motion based on (8). The robot's head oscillates with variable amplitude, A_θ, and offset, ϵ, controlled by a user. The light blue area represents the range of oscillation while the red line shows the robot's current head angle with respect to the previous module.

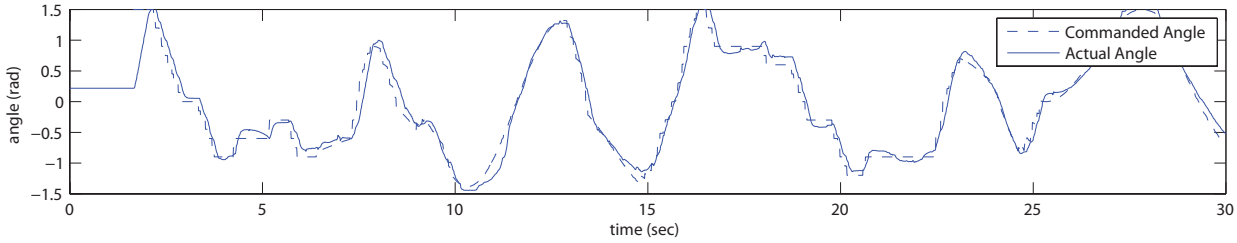

Fig. 12: Commanded and feedback data from the robot's head module for the trial shown in Fig. 11. Note that the head tracks the commanded joint angle relatively stiffly, while the rest of the robot is compliant because the shape is propagated solely through torque control.

[9] G. Chirikjian and J. Burdick, "A modal approach to hyper-redundant manipulator kinematics," *IEEE Transactions on Robotics and Automation*, vol. 10, pp. 343–354, June 1994.

[10] J. Burdick, J. Radford, and G. Chirikjian, "A Sidewinding Locomotion Gait for Hyper-Redundant Robots," *Robotics and Automation*, vol. 3, pp. 101–106, 1993.

[11] A. A. Transeth, K. Y. Pettersen, and P. l. Liljebäck, "A survey on snake robot modeling and locomotion," *Robotica*, vol. 27, p. 999, Mar. 2009.

[12] D. Rollinson, S. Ford, B. Brown, and H. Choset, "Design and Modeling of a Series Elastic Element for Snake Robots," in *ASME Dynamic Systems and Control Conference (DSCC)*, (Palo Alto, USA), 2013.

[13] G. Pratt and M. Williamson, "Series elastic actuators," *Proceedings 1995 IEEE/RSJ International Conference on Intelligent Robots and Systems.*, pp. 399–406, 1995.

[14] H. Yamada and S. Hirose, "Study on the 3D shape of active cord mechanism," in *IEEE International Conference on Robotics and Automation (ICRA)*, (Orlando, USA), pp. 2890–2895, IEEE, 2006.

[15] A. J. Ijspeert, J. Nakanishi, and S. Schaal, "Learning attractor landscapes for learning motor primitives," *Advances in Neural Information Processing Systems*, vol. 15, pp. 1523–1530, 2002.

[16] A. Fod, M. Matarić, and O. Jenkins, "Automated derivation of primitives for movement classification," *Autonomous Robots*, vol. 12, no. 1, pp. 39–54, 2002.

[17] H. Date and Y. Takita, "Adaptive locomotion of a snake like robot based on curvature derivatives," in *IEEE/RSJ International Conference on Intelligent Robots and Systems (IROS)*, (San Diego, USA), pp. 3554–3559, IEEE, Oct. 2007.

[18] T. Kano and A. Ishiguro, "Obstacles are beneficial to me! Scaffold-based locomotion of a snake-like robot using decentralized control," in *2013 IEEE/RSJ International Conference on Intelligent Robots and Systems*, (Tokyo, Japan), pp. 3273–3278, IEEE, Nov. 2013.

[19] T. Kamegawa, R. Kuroki, M. Travers, and H. Choset, "Proposal of EARLI for the snake robot's obstacle aided locomotion," *2012 IEEE International Symposium on Safety, Security, and Rescue Robotics (SSRR)*, Nov. 2012.

[20] D. Rollinson and H. Choset, "Virtual Chassis for Snake Robots," in *IEEE/RSJ International Conference on Intelligent Robots and Systems (IROS)*, (San Francisco, USA), 2011.

[21] D. Rollinson, H. Choset, and S. Tully, "Robust State Estimation with Redundant Proprioceptive Sensors," in *ASME Dynamic Systems and Control Conference (DSCC)*, (Palo Alto, USA), 2013.

[22] D. I. Goldman and D. L. Hu, "Wiggling Through the World: The mechanics of slithering locomotion depend on the surroundings," *American Scientist*, pp. 314–323, 2010.